6

Hydrological processes in the Blue Nile

Zachary M. Easton, Seleshi B. Awulachew, Tammo S. Steenhuis, Saliha Alemayehu Habte, Birhanu Zemadim, Yilma Seleshi and Kamaleddin E. Bashar

Key messages

- While we generally have a fundamental understanding of the dominant hydrological processes in the Blue Nile Basin, efforts to model it are largely based on temperate climate hydrology. Hydrology in the Blue Nile Basin is driven by monsoonal climate, characterized by prolonged wet and dry phases, where run-off increases as the rainy season (which is also the growing season) progresses. In temperate climates, run-off typically decreases during the growing season as plants remove soil moisture. In the Blue Nile Basin there is a threshold precipitation level needed to satisfy soil-moisture capacity (approximately 500 mm) before the basin begins to generate run-off and flow.
- Not all areas of the basin contribute equally to Blue Nile flow. Once the threshold moisture content is reached, run-off generation first occurs from localized areas of the landscape that become saturated or are heavily degraded. These saturated areas are often found at the bottom of large slopes, or in areas with a large upslope-contributing area, or soils with a low available soil moisture storage capacity. As the monsoonal season progresses, other areas of the basin with greater soil moisture storage capacity begin to contribute to run-off. By the end of the monsoon, more than 50 per cent of the precipitation can end up as run-off. This phenomenon is termed 'saturation excess run-off' and has important implications for identifying and locating management practices to reduce run-off losses.
- The Soil and Water Assessment Tool (SWAT) model is modified to incorporate these run-off dynamics, by adding a landscape-level water balance. The water balance version of SWAT (SWAT-WB) calculates the water deficit (e.g. available soil moisture storage capacity) for the soil profile for each day, and run-off is generated once this water deficit is satisfied. We show that this conceptualization better describes hydrological processes in the Blue Nile Basin.
- Models that include saturation excess (such as our adaptation to the SWAT model) are not only able to simulate the flow well but also good in predicting the distribution of run-off in the landscape. The latter is extremely important when implementing soil and water conservation practices to control run-off and erosion in the Blue Nile Basin. The SWAT-WB model shows that these practices will be most effective if located in areas with convergent topography.

Overview

This chapter provides an analysis of the complexity of hydrological processes using detailed studies at scales from the micro-watershed to the Blue Nile Basin (BNB). Data collected from various sources include long-term Soil Conservation Reserve Program (SCRP) data (Hurni, 1984), and consist of both hydrological data in the form of streamflow and stream sediment concentrations and loads. Data collected by students in the SCRP watersheds include piezometric water table data and plot studies of run-off dynamics. Governmental and non-governmental sources provided meteorological data, as well as data on land use, elevation and soil inputs for modelling analysis. In the small SCRP watersheds, the analysis focused on piezometric water table data and run-off losses as they relate to the topographic position in the watershed. In parallel, basin-scale models were used to enhance understanding of rainfall run-off and erosion processes and the impact of management interventions on these processes in the BNB.

Introduction

A better understanding of the hydrological processes in the headwaters of the BNB is of considerable importance because of the trans-boundary nature of the BNB water resources. Ethiopia has abundant, yet underutilized, water resource potential, and 3.7 million ha of potentially irrigable land that can be used to improve agricultural production (MoWR, 2002; Awulachew *et al.*, 2007). Yet only 5 per cent of Ethiopia's surface water (0.6% of the Nile Basin's water resource) is being currently utilized by Ethiopia (Arseno and Tamrat, 2005). Sudan receives most of the flow leaving the Ethiopian Highlands, and has considerable infrastructure in the form of reservoirs and irrigation schemes that utilize these flows. Ethiopian Highlands are the source of more than 60 per cent of the Nile flow (Ibrahim, 1984; Conway and Hulme, 1993). This proportion increases to almost 95 per cent during the rainy season (Ibrahim, 1984). However, agricultural productivity in Ethiopia lags behind other similar regions, which is attributed to unsustainable environmental degradation mainly from erosion and loss of soil fertility (Grunwald and Norton, 2000). In addition, there is a growing concern about how climate and human-induced degradation will impact the BNB water resources (Sutcliffe and Parks, 1999), particularly in light of limited hydrological and climatic studies in the basin (Arseno and Tamrat, 2005).

One characteristic of Ethiopian BNB hill slopes is that most have infiltration rates in excess of the rainfall intensity. Consequently, most run-off is produced when the soil saturates (Ashagre, 2009) or from shallow, degraded soils. Engda (2009) showed that the probability of rainfall intensity exceeding the measured soil infiltration rate is 8 per cent. This is not to imply that infiltration excess, or Hortonian flow (Horton, 1940), is not present in the basin, but that it is not the dominant hydrological process. Indeed, Steenhuis *et al.* (2009) and Collick *et al.* (2009) not only note the occurrence of infiltration excess run-off but also state that it is predominantly found in areas with exposed bedrock or in extremely shallow and degraded soils. Most of the models utilized to assess the hydrological response of basins such as the BNB are arguably incorrect (or at the very least incomplete) in their ability to adequately simulate the complex interrelations of climate, hydrology and human impacts. This is not because the models are poorly constructed but often because they were developed and tested in very different climates, locations and hydrological regimes. Indeed, most hydrological models have been developed in, and tested for, conditions typical of the United States or Europe (e.g. temperate climate, with an even distribution of rainfall), and thus lack the fundamental understanding of

how regions dominated by monsoonal conditions (such as the BNB) function hydrologically. Thus, a paradigm shift is needed on how the hydrological community conceptualizes hydrological processes in these data-scarce regions.

In monsoonal climates a given rainfall volume at the onset of the monsoon produces a different run-off volume than the same rainfall at the end of the monsoon (Lui *et al.*, 2008). Lui *et al.* (2008) and Steenhuis *et al.* (2009) showed that the ratio of discharge to precipitation minus evapotranspiration (Q/(P – ET)) increases with cumulative precipitation from the onset of the monsoon and, consequently, the watersheds behave differently depending on the amount of stored moisture, suggesting that saturation excess processes play an important role in the watershed run-off response. Other studies in the BNB or nearby catchments have suggested that saturation excess processes control overland flow generation (Collick *et al.*, 2009; Ashagre, 2009; Engda, 2009; Tebebu, 2009; Easton *et al.*, 2010; Tebebu *et al.*, 2010; White *et al.*, 2011) and that infiltration-excess run-off is rare (Liu *et al.*, 2008; Engda, 2009).

Many of the commonly used watershed models employ some form of the Soil Conservation Service curve number to predict run-off, which links run-off response to soils, land use and five-day antecedent rainfall (AMC), and not the cumulative seasonal rainfall volume. The Soil and Water Assessment Tool (SWAT) model is a basin-scale model where run-off is based on land use and soil type (Arnold *et al.*, 1998), and not on topography. As a result, run-off and sediment transport on the landscape are only correctly predicted for infiltration excess of overland flow, and not when saturation excess of overland flow from variable source areas (VSA) dominates. Thus, critical landscape sediment source areas might not be explicitly recognized.

The analysis in this chapter utilizes existing data sets to describe the hydrological characteristics of the BNB with regard to climatic conditions, rainfall characteristics and run-off process across various spatial scales in the BNB. An attempt is made to explain the processes governing the generation of run-off at various scales in the basin, from the small watershed to the basin level and to quantify the water resources at these scales. Models used to predict the source, timing and magnitude of run-off in the basin are reviewed, the suitability and limitations of existing models are described, and approaches and results of newly derived models are presented.

Much of the theory of run-off production that follows is based on, and corroborated by, studies carried out in the SCRP watersheds. These micro-watersheds are located in headwater catchments in the basin and typify the landscape features of much of the highlands, and are thus somewhat hydrologically representative of the basin. A discussion of the findings from these SCRP micro-watersheds is followed by work done in successively larger basins (e.g. watershed, sub-basin and basin) and, finally, by an attempt to integrate these works using models across the various scales.

Rainfall run-off processes

Micro-watershed hydrological processes

SCRP watersheds have the longest and most accurate record of both rainfall and run-off data available in Ethiopia. Three of the sites are located in the Amhara region either in or close to the Nile Basin: Andit Tid, Anjeni and Maybar (SCRP, 2000). All three sites are dominated by agriculture, with control structures built for soil erosion to assist the rain-fed subsistence farming (Table 6.1).

Table 6.1 Location, description and data span from the three SCRP research sites

Site	*Watershed centroid (region)*	*Area (ha)*	*Elevation range (masl)*	*Precipitation (mm yr^{-1})*	*Length of record*
Andit Tid	39°43' E, 9°48' N (Shewa)	477.3	3040–3548	1467	1987–2004 (1993, 1995–1996 incomplete)
Anjeni	37°31' E, 10°40' N (Gojam)	113.4	2407–2507	1675	1988–1997
Maybar	37°31' E, 10°40' N (South Wollo)	112.8	2530–2858	1417	1988–2001 (1990–1993 incomplete)

The Andit Tid Research Unit covers a total area of 481 ha with an elevation of 3040–3548 m, with steep and degraded hill slopes (Bosshart, 1997), resulting in 54 per cent of the long-term precipitation becoming run-off (Engda, 2009). Conservation practices including terraces, contour drainage ditches and stone bunding have been installed to promote infiltration and reduce soil loss. In addition to long-term rainfall run-off and meteorological measurements, plot-scale measures of soil infiltration rate at 10 different locations throughout the watershed were taken and geo-referenced with a geographic positioning system (GPS). Soil infiltration was measured using a single-ring infiltrometer of 30 cm diameter.

The Anjeni watershed is located in the Amhara Region of the BNB. The Anjeni Research Unit covers a total area of 113 ha and is the most densely populated of the three SCRP watersheds, with elevations from 2400 to 2500 m. The watershed has extensive soil and water conservation measures, mainly terraces and small contour drainage ditches. From 1987 to 2004 rainfall was measured at five different locations, and discharge was recorded at the outlet and from four run-off plots. Of the rainfall, 45 per cent becomes run-off. During the 2008 rainy season the soil infiltration rate was measured at ten different locations throughout the watershed using a single-ring infiltrometer of 30 cm diameter. In addition, piezometers were installed in transects to measure the water table depths.

The 112.8 ha Maybar catchment was the first of the SCRP research sites, characterized by rugged topography with slopes ranging between 2530 and 2860 m. Rainfall and flow data were available from 1988 to 2004. Discharge was measured with a flume installed in the Kori River using two methods: float-actuated recorder and manual recording. The groundwater table levels were measured with 29 piezometers located throughout the watershed. The saturated area in the watershed was delineated and mapped using a combination of information collected using a GPS, coupled with field observation and groundwater-level data.

Analysis of rainfall discharge data in SCRP watersheds

To investigate run-off response patterns, discharges in the Anjeni, Andit Tid and Maybar catchments were plotted as a function of effective rainfall (i.e. precipitation minus evapotranspiration, P – E) during the rainy and dry seasons. In Figure 6.1a an example is given for the Anjeni catchment. As is clear from this figure, the watershed behaviour changes as the wet season progresses, with precipitation later in the season generally producing a greater percentage of run-off. As rainfall continues to accumulate during the rainy season, the

watershed eventually reaches a threshold point where run-off response can be predicted by a linear relationship with effective precipitation, indicating that the proportion of the rainfall that became run-off was constant during the remainder of the rainy season. For the purpose of this study, an approximate threshold of 500 mm of effective cumulative rainfall (P – E) was determined after iteratively examining rainfall/run-off plots for each watershed. The proportion Q/(P – E) varies within a relatively small range for the three SCRP watersheds, despite their different characteristics. In Anjeni, approximately 48 per cent of late season effective rainfall became run-off, while ratios for Andit Tid and Maybar were 56 and 50 per cent, respectively (Liu *et al.*, 2008). There was no correlation between biweekly rainfall and discharge during the dry seasons at any of the sites.

Despite the great distances between the watersheds and the different characteristics, the response was surprisingly similar. The Anjeni and Maybar watersheds had almost the same run-off characteristics, while Andit Tid had more variation in the run-off amounts but, on average, the same linear response with a higher intercept (Figure 6.1b). Linear regressions were generated for all three watersheds (Figures 6.1). The regression slope does not change significantly, but this is due to the more similar values in Anjeni and Maybar dominating the fit (note that these regressions are only valid for the end of rainy seasons when the watersheds are wet).

Why these watersheds behave so similarly after the threshold rainfall has fallen is an interesting characteristic to explore. It is imperative to look at various time scales, since focusing on just one type of visual analysis can lead to erroneous conclusions. For example, looking only at storm hydrographs of the rapid run-off responses prevalent in Ethiopian storms, one could conclude that infiltration excess is the primary mechanism generating run-off. However, looking at longer time scales it can be seen that the ratio of Q/(P – E) is increasing with cumulative precipitation and, consequently, the watersheds behave differently depending on how much moisture is stored in the watershed, suggesting that saturation excess processes play an important role in the watershed run-off response. If infiltration excess was controlling run-off responses, discharge would only depend on the rate of rainfall, and there would be no clear relationship with antecedent cumulative precipitation, as is clearly the case as shown in Figure 6.1.

Infiltration and precipitation intensity measurements

To further investigate the hydrological response in the SCRP watersheds, the infiltration rates are compared with rainfall intensities in the Maybar (Figure 6.2a) and Andit Tid (Figure 6.2b) watersheds, where infiltration rates were measured in 2008 by Bayabil (2009) and Engda (2009), and rainfall intensity records were available from the SCRP project for the period 1986–2004. In Andit Tid, the exceedance probability of the average intensities of 23,764 storm events is plotted in Figure 6.2b (blue line). These intensities were calculated by dividing the rainfall amount on each day by the duration of the storm. In addition, the exceedance probability for instantaneous intensities for short periods was plotted as shown in Figure 6.2b (red line). Since there are often short durations of high-intensity rainfall within each storm, the rainfall intensities for short periods exceeded those of the storm-averaged intensities as shown in Figure 6.2b.

The infiltration rates for 10 locations in Andit Tid measured with the diameter single-ring infiltrometer varied between a maximum of 87 cm hr^{-1} on a terraced eutric cambisol in the bottom of the watershed to a low of 2.5 cm hr^{-1} on a shallow sandy soil near the top of the hill slope. This low infiltration rate was mainly caused by the compaction of freely roaming animals for grazing. Bushlands, which are dominant on the upper watershed, have significantly

a

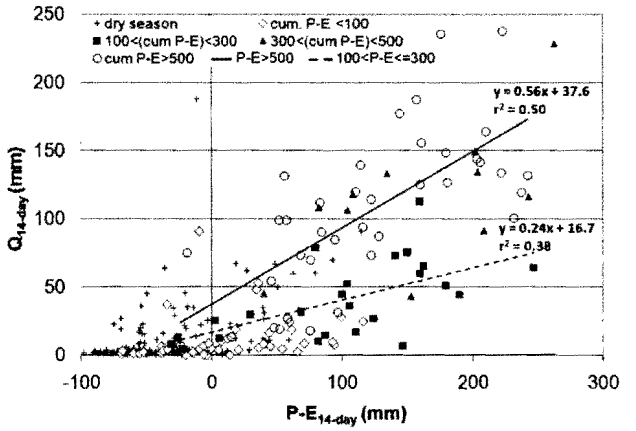

b

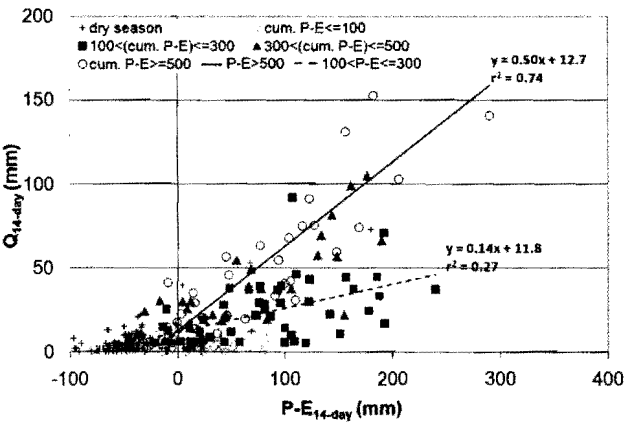

c

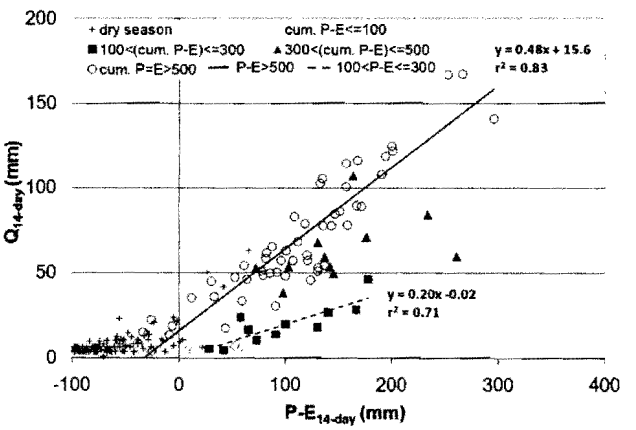

Figure 6.1 Biweekly summed rainfall/discharge relationships for (a) Andit Tid, (b) Anjeni and (c) Maybar. Rainy season values are grouped according to the cumulative rainfall that had fallen during a particular season, and a linear regression line is shown for the wettest group in each watershed

Source: Lui *et al.*, 2008

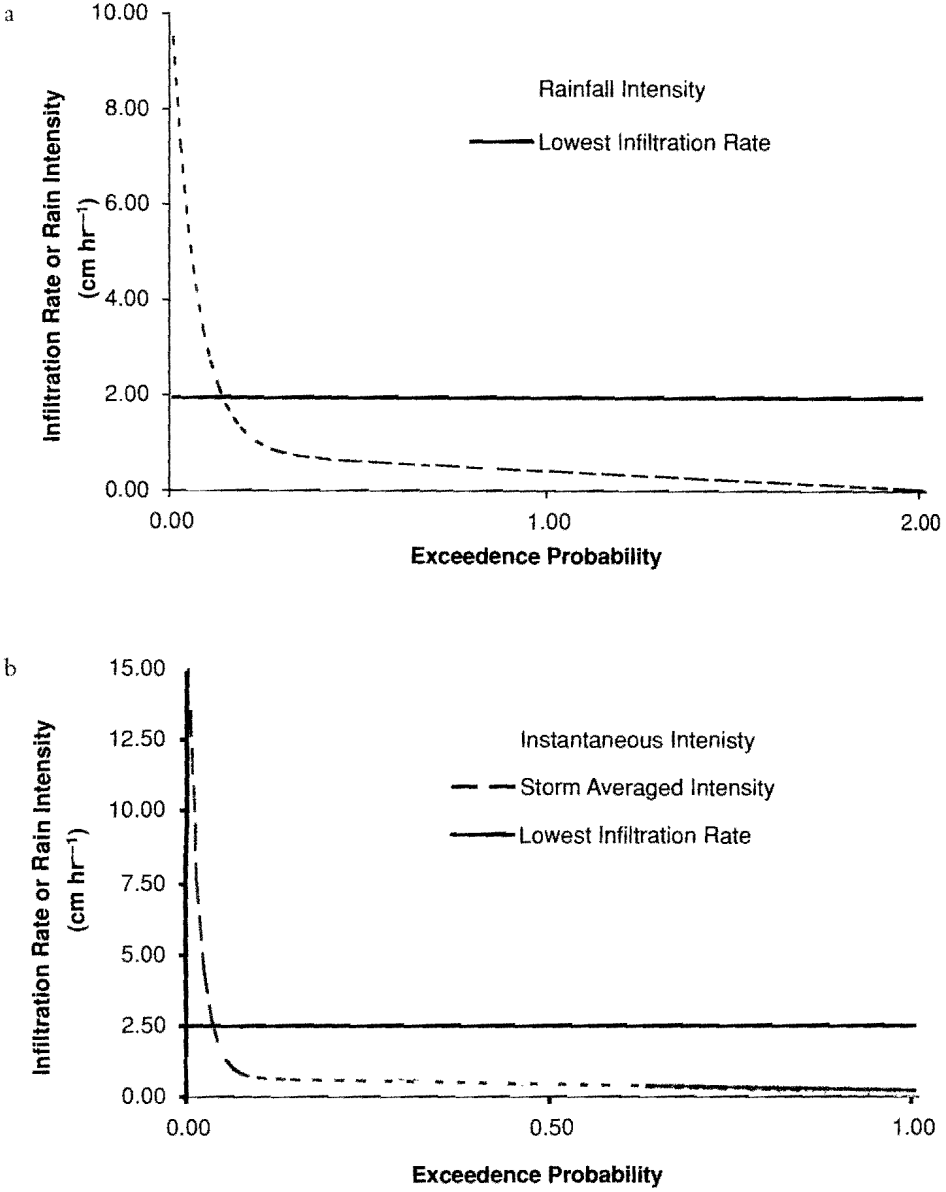

Figure 6.2 Probability of soil infiltration rate being exceeded by a five-minute rainfall intensity for the (a) Andit Tid and (b) Anjeni watersheds. Horizontal lines indicate the lowest measured infiltration rate

higher infiltration rates. In general, terraced and cultivated lands also have higher infiltration rates. The average infiltration rate of all ten measurements of the storm intensities was 12 cm hr^{-1}, and the median 4.3 cm hr^{-1}. The median infiltration rate of 4.3 cm hr^{-1} is the most meaningful value to compare with the rainfall intensity since it represents a spatial average. This

median intensity has an exceedance probability of 0.03 for the actual storm intensities and 0.006 for the storm-averaged intensities. Thus the median intensity was exceeded only 3 per cent of the time and for less than 1 per cent of the storms. Storms with greater intensities were all of short duration with amounts of less than 1cm of total precipitation except once when almost 4 cm of rain fell over a 40-minute period. The run-off generated during short-duration intense rainfall can infiltrate into the soil in the subsequent period in the soil down slope when the rainfall intensity is less or the rain has stopped.

A similar analysis was performed in the Maybar watershed (Derib, 2005), where 16 infiltration rates were measured and even greater infiltration rates than in Andit Tid were found. The final steady state infiltration rates ranged from 1.9 to 60 cm hr^{-1}, with a median of 17.5 cm hr^{-1} (Figure 6.2a). The steady state infiltration rates in the Maybar watershed (Derib, 2005) ranged from 19 to 600 mm hr^{-1}. The average steady state infiltration rate of all 16 measurements was 24 cm h^{-1} and the median was 18 cm hr^{-1}. The median steady state infiltration rate (or geometric mean) was 18 cm hr^{-1}. The average daily rainfall intensity for seven years (from 1996 to 2004) was 8.5 mm hr^{-1}. A comparison of the geometric mean infiltration rate with the probability that a rainfall intensity of the same or greater magnitude occurs showed that the median steady state infiltration rate is not exceeded, while the minimum infiltration rate is exceeded only 9 per cent of the time. Thus, despite the rapid observed increase in flow at the outlet of the watershed during a rainstorm, it is unlikely that high rainfall intensities caused infiltration excess run-off, and more likely that saturated areas contributed the majority of the flow. Locally, there can be exceptions. For example, when the infiltration rate is reduced or in areas with severe degradation, livestock traffic can cause infiltration excess run-off (Nyssen *et al.*, 2010). Thus, the probability of exceedence is approximately the same as in Andit Tid, despite the higher rainfall intensities.

These infiltration measurements confirm that infiltration excess run-off is not a common feature in these watersheds. Consequently, most run-off that occurs in these watersheds is from degraded soils where the topsoil is removed or by saturation excess in areas where the upslope interflow accumulates. The finding that saturation excess is occurring in watersheds with a monsoonal climate is not unique. For example, Bekele and Horlacher (2000), Lange *et al.* (2003), Hu *et al.* (2005) and Merz *et al.* (2006) found that saturation excess could describe the flow in a monsoonal climate in southern Ethiopia, Spain, China and Nepal, respectively.

Piezometers and groundwater table measurements

In all three SCRP watersheds, transects of piezometers were installed to observe groundwater table in 2008 during the rainy reason and the beginning of the dry season.

Both Andit Tid and Maybar had hill slopes with shallow- to medium-depth soils (0.5–2.0 m depth) above a slow sloping permeable layer (either a hardpan or bedrock). Consequently, the water table height above the slowly permeable horizon (as indicated by the piezometers) behaved similarly for both watersheds. An example is given for the Maybar watershed, where groundwater table levels were measured with 29 piezometers across eight transects (Figure 6.3). The whole watershed was divided into three slope ranges: upper steep slope (25.1–53.0°), mid-slope (14.0–25.0°) and relatively low-lying areas (0–14.0°). For each slope class the daily perched groundwater depths were averaged (i.e. the height of the saturated layer above the restricting layer). The depth of the perched groundwater above the restricting layer in the steep and upper parts of the watershed is very small and disappears if there is no rain for a few days. The depth of the perched water table on the mid-slopes is greater than that of the upslope areas. The perched groundwater depths are, as expected, the greatest in relatively low-lying

areas. Springs occur at the locations where the depth from the surface to the impermeable layer is the same as the depth of the perched water table and are the areas where the surface run-off is generated.

The behaviour of water table is consistent with what one would expect if interflow is the dominant conveyance mechanism. *Ceteris paribus*, the greater the driving force (i.e. the slope of the impermeable layer), the smaller the perched groundwater depth needed to transport the same water because the lateral hydraulic conductivity is larger. Moreover, the drainage area and the discharge increase with the downslope position. Consequently, one expects the perched groundwater table depth to increase with the downslope position as both slopes decrease and drainage area increases.

These findings are different from those generally believed to be the case – that the vegetation determines the amount of run-off in the watershed. Plotting the average daily depth of the perched water table under the different crop types (Figure 6.3a) revealed a strong correlation between perched water depth and crop type. The grassland had the greatest perched water table depth, followed by croplands, while bushlands had the lowest groundwater level. However, some local knowledge was needed to interpret these data. For instance, the grasslands are mainly located in the often-saturated lower-lying areas (too wet to grow a crop), while the croplands are often located in the mid-slope (with a consistent water supply but not saturated) and the bushlands are found on the upper steep slope areas (too droughty for good yield). Since land use is related to slope class (Figure 6.3b), the same relationship between crop type and soil water table height is not expected to be seen as between slope class and water table height. Thus there is an indirect relationship between land use and hydrology. The landscape determines the water availability, and thus the land use.

In the Anjeni watershed, which had relatively deep soils and no flat-bottom land, the only water table found was near the stream. The water table level was above the stream level, indicating that the rainfall infiltrates first in the landscape and then flows laterally to the stream. Although more measurements are needed it seems reasonable to speculate that there was a portion of the watershed that had a hardpan at a shallow depth with a greater percolation rate than in either Andit Tid or Maybar allowing recharge but, at the same time, causing interflow and saturation excess overland flow.

Perhaps the most interesting interplay between soil water dynamics and run-off source areas can be observed in the Maybar catchment. For instance, transect 1 illustrates a typical water table response across slope classes in the catchment. This and other transects have a slow permeable layer (either a hardpan or bedrock) and the water tends to pond above this layer.

At the beginning of August (the middle of the rainy season) the water table at the most down-slope location, P1, increased and reached the surface of the soil on 17 August (Figure 6.4). On a few dates, it was located even above the surface indicating surface run-off at the time. The water table started declining at the end of September, when precipitation ceased. The water level in P2, located upslope of P1, reached its maximum on 29 August, and the level remained below the surface. It decreased around the beginning of September, when rainfall storms were less frequent (Figure 6.4). The water table in P3 responded quickly and decreased rapidly. Thus, unlike P1 and P2, the water did not accumulate there and flowed rapidly as interflow downslope. Finally, the response time in the most upstream piezometer, P4, was probably around the duration of the rainstorm and was not recorded by our manual measurements.

Thus, the piezometric data in this and other transects indicate that the rainfall infiltrates on the hillsides and flows laterally as interflow down slope. At the bottom of the hillside where the slope decreases, the water accumulates and the water table increases. When the water intersects

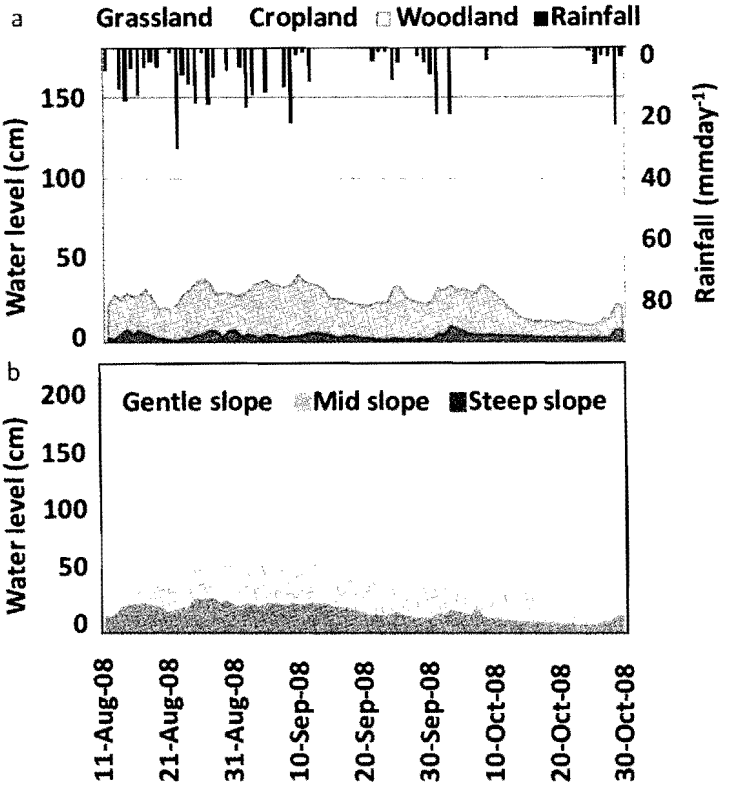

Figure 6.3 Average daily water level for three land uses (i.e. grasslands, croplands and woodlands) calculated above the impermeable layer superimposed (a) with daily rainfall and (b) for three slope classes in the Maybar catchment

with the soil surface, a saturated area is created. Rainfall on this saturated area becomes overland flow. In addition, rainfall at locations where the water table remains steady, such as P2, also becomes run-off; otherwise it would rise to the surface. Natural soil pipes that rapidly convey water from the profile and that have been seen in many places in this watershed might be responsible for this process (Bayabil, 2009).

These findings indicate that topographic controls are important to consider when assessing watershed response. However, when the average daily depth of the perched water table is plotted against the different crop types (e.g. Figure 6.3a), there was also a strong correlation of perched water depth with crop type. The grasslands at the bottom of the slope had the greatest perched water table depth, followed by croplands and woodlands with the lowest groundwater level. Thus, it seems that similar to the plot data, both ecological factors and topographical factors play a role in determining the perched water table height. Since land use is related to slope class, the same relationship between crop type and soil water table height as slope class and water table height is expected. Thus, there is an indirect relationship between land use and hydrology. The landscape determines the water availability and thus the land use.

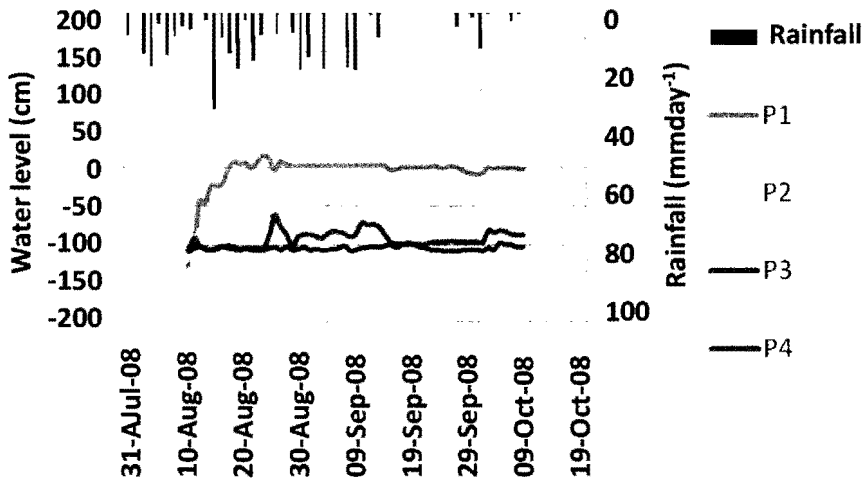

Figure 6.4 Piezometric water-level data transect 1 in the upper part of the watershed, where the slope is even. Water level was measured twice a day during the 2008 main rainy season using the ground surface as a reference and rainfall as a daily measurement

The results of this study are similar to those of the May Zeg watershed, which is in a much dryer area in Tigrai, with an average annual rainfall of around 600 mm yr^{-1} (Nyssen *et al.*, 2010). In this study, the water table in the valley bottom was measured with a single piezometer. Nyssen *et al.* (2010) observed that increasing infiltration on the hillside resulted in a faster increase in water tables in the valley bottom, which is similar to what was observed in the Maybar catchment where water moved via the subsurface, which increased the water levels where the slope decreased.

Thus, although there is a relationship between run-off potential and crop type, the relationship is indirect. The saturated areas are too wet for a crop to survive and these areas are often left as grass. The middle slopes have sufficient moisture (and do not saturate) to survive the dry spells in the rainy season. The steep slopes, without any water table, are likely to be droughty for a crop to survive during dry years and are therefore mainly forest or shrub.

These findings are consistent with the measurements taken by McHugh (2006) in the Lenche Dima watershed near Woldea, where the surface run-off of the valley bottom lands were much greater than the run-off (and erosion) from the hillsides.

Run-off from test plots

The rainfall run-off data collected from run-off plots in the Maybar watershed for the years 1988, 1989, 1992 and 1994 allow further identification of the dominant run-off processes in the watershed. The average annual run-off measured on four plots showed that plots with shallower slopes had higher run-off losses than those with steeper slopes (Figure 6.5a). The run-off coefficients ranged from 0.06 to 0.15 across the slope classes (Figure 6.5a). Nyssen *et al.* (2010) compiled the data of many small run-off plots in Ethiopia and showed an even larger range of

run-off coefficients across slope classes. Run-off from plots in the Andit Tid catchment showed a very similar slope response (Figure 6.5b) as the Maybar plots, with shallower slopes producing more run-off. These results indicate that the landscape position plays an important role in the magnitude of the run-off coefficients as well. Indeed, it is commonly accepted that, ceteris paribus, a greater slope causes an increase in the lateral hydraulic conductivity of the soils, and thus these soils maintain a greater transmissivity than shallower slopes, and are able to conduct water out of the profile faster, reducing run-off losses.

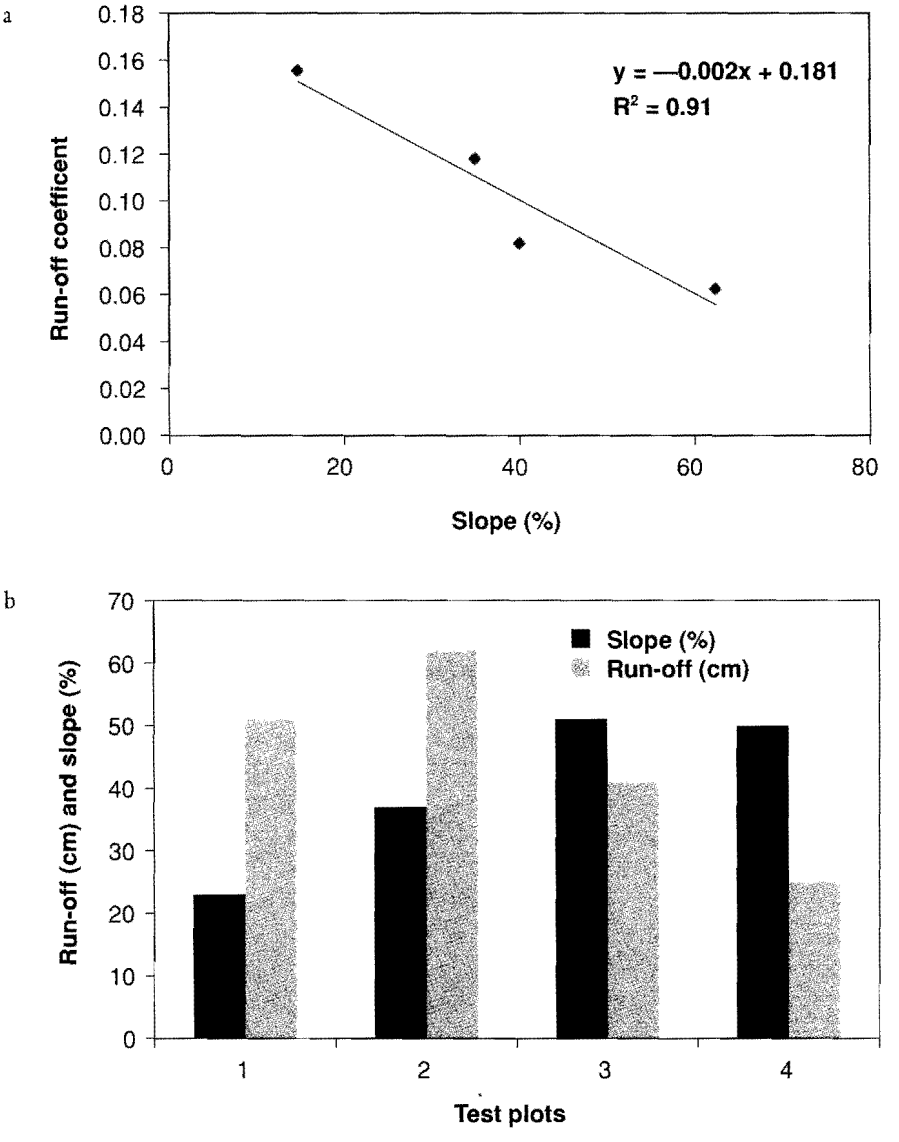

Figure 6.5 Plot run-off coefficient computed from daily 1988, 1989, 1992 and 1994 rainfall and run-off data for different slopes in (a) the Maybar catchment and (b) run-off depths for various slope classes in the Andit Tid catchment

Discussion

Both the location of run-off source areas and the effectiveness of a soil and water conservation practice depend on the dominating run-off processes in the watershed. Whether watershed run-off processes are ecologically (plant) or topographically controlled is an important consideration when selecting appropriate practices. Inherent in the assumption of ecologically based run-off is the concept of soil infiltration excess type of overland flow in which run-off occurs when rainfall intensity exceeds the infiltration capacity of the soil. Thus, for ecologically based models, improving plant cover and soil health will, in general, reduce overland flow and increase infiltration and interflow. On the other hand, topographically based run-off processes are, in general, based on the principle that if the soil saturates either above a slow permeable layer or a groundwater table, run-off occurs. In this case, changing plant cover will have little effect on run-off unless the conductivity of the most restricting layer is altered. These areas, which saturate easily, are called run-off source areas. They indicate where soil and water conservation practices would be most effective because most of the erosion originates in these areas. Understanding hydrological processes of a basin as diverse as the BNB is an essential prerequisite to understand the water resources and to ultimately design water management strategies for water access and improve water use in agriculture and other sectors. The results of various studies as briefly demonstrated above provide a wide range of tools and methods of analysis to explain such process. These finding will assist water resources and agricultural planners, designers and managers with a tool to better manage water resources in Ethiopian Highlands and to potentially mitigate impacts on water availability in downstream countries.

These results from the SCRP watersheds serve as the basis for the adoption of the models discussed next.

Adoption of models to the Blue Nile

Watershed management depends on the correct identification of when and where run-off and pollutants are generated. Often, models are utilized to drive management decisions, and focus resources where they are most needed. However, as discussed above, the hydrology and, by extension, biogeochemical processes in basins such as the Blue Nile, dominated by monsoonal conditions, often do not behave in a similar manner as watersheds elsewhere in the world. As a result, the models utilized to assess hydrology often do not correctly characterize the processes, or require excessive calibration and/or simplifying assumptions. Thus, watershed models that are capable of capturing these complex processes in a dynamic manner can be used to provide an enhanced understanding of the relationship between hydrological processes, erosion/sedimentation and management options.

There are many models that can continuously simulate streamflow, erosion/sedimentation or nutrient loss from a watershed. However, most were developed in temperate climates and were never intended to be applied in monsoonal regions, such as Ethiopia, with an extended dry period. In monsoonal climates, a given rainfall volume at the onset of the monsoon produces a drastically different run-off volume than the same rainfall volume at the end of the monsoon (Lui *et al.*, 2008).

Many of the commonly used watershed models employ some form of the Soil Conservation Service curve number (CN) to predict run-off, which links run-off response to soils, land use and five-day antecedent rainfall (e.g. antecedent moisture condition, AMC), and not the cumulative seasonal rainfall volume. The SWAT model is a basin-scale model where run-off is based on land use and soil type (Arnold *et al.*, 1998), and not on topography; therefore, run-off and

sediment transport on the landscape are only correctly predicted for soil infiltration excess type of overland flow and not when saturation excess of overland flow from variable source areas (VSA) dominates. Thus critical sediment source areas might not be explicitly recognized as unique source areas. SWAT determines an appropriate CN for each simulated day by using this CN–AMC distribution in conjunction with daily soil moisture values determined by the model. This daily CN is then used to determine a theoretical storage capacity, S, of the watershed for each day. While a theoretical storage capacity is assigned and adjusted for antecedent moisture for each land use/soil combination, the storage is not used to directly determine the amount of water allowed to enter the soil profile. Since this storage is a function of the land's infiltration properties, as quantified by the CN–AMC, SWAT indirectly assumes that only infiltration excess processes govern run-off generation. Prior to any water infiltrating, the exact portion of the rainfall that will run-off is calculated via these infiltration properties. This determination of run-off volume before soil water volume is an inappropriate approach for all but the most intense rain events, particularly in monsoonal climates where rainfall is commonly of both low intensity and long duration and saturation processes generally govern run-off production. Several studies in the BNB or nearby watersheds have suggested that saturation excess processes control overland flow generation (Liu *et al.*, 2008; Collick *et al.*, 2009; Ashagre, 2009; Engda, 2009; Tebebu, 2009; Tebebu *et al.*, 2010; White *et al.*, 2011) and that infiltration excess run-off is rare (Liu *et al.*, 2008; Engda, 2009).

Many have attempted to modify the CN to better work in monsoonal climates, by proposing various temporally based values and initial abstractions. For instance, Bryant *et al.* (2006) suggest that a watershed's initial abstraction should vary as a function of storm size. While this is a valid argument, the introduction of an additional variable reduces the appeal of the one-parameter CN model. Kim and Lee (2008) found that SWAT was more accurate when CN values were averaged across each day of simulation, rather than using a CN that described moisture conditions only at the start of each day. White *et al.* (2009) showed that SWAT model results improved when the CN was changed seasonally to account for watershed storage variation due to plant growth and dormancy. Wang *et al.* (2008) improved SWAT results by using a different relationship between antecedent conditions and watershed storage. While these variable CN methods improve run-off predictions, they are not easily generalized for use outside of the watershed as they are tested mainly because the CN method is a statistical relationship and is not physically based.

In many regions, surface run-off is produced by only a small portion of a watershed that expands with an increasing amount of rainfall. This concept is often referred to as a variable source area (VSA), a phenomenon actually envisioned by the original developers of the CN method (Hawkins, 1979), but never implemented in the original CN method as used by the Natural Resource Conservation Service (NRCS). Since the method's inception, numerous attempts have been made to justify its use in modelling VSA-dominated watersheds. These adjustments range from simply assigning different CNs for wet and dry portions to correspond with VSAs (Sheridan and Shirmohammadi, 1986; White *et al.*, 2009), to full reinterpretations of the original CN method (Hawkins, 1979; Steenhuis *et al.*, 1995; Schneiderman *et al.*, 2007; Easton *et al.*, 2008).

To determine what portion of a watershed is producing surface run-off for a given precipitation event, the reinterpretation of the CN method presented by Steenhuis *et al.* (1995) and incorporated into SWAT by Easton *et al.* (2008) assumes that rainfall infiltrates when the soil is unsaturated or runs off when the soil is saturated. It has been shown that this saturated contributing area of a watershed can be accurately modelled spatially by linking this reinterpretation of the CN method with a topographic index (TI), similar to those used by the topographically driven TOPMODEL (Beven and Kirkby, 1979; Lyon *et al.*, 2004). This linked

CN–TI method has since been used in multiple models of watersheds in the north-eastern US, including the Generalized Watershed Loading Function (GWLF; Schneiderman *et al.*, 2007) and SWAT (Easton *et al.*, 2008). While the reconceptualized CN model is applicable in temperate US climates, it is limited by the fact that it imposes a distribution of storages throughout the watershed that need to fill up before run-off occurs. While this limitation does not seem to affect results in temperate climates, it results in poor model results in monsoonal climates.

SWAT–VSA, the CN–TI adjusted version of SWAT (Easton *et al.*, 2008), returned hydrological simulations as accurate as the original CN method; however, the spatial predictions of run-off-producing areas and, as a result, the predicted phosphorus export were much more accurate. While SWAT–VSA is an improvement upon the original method in watersheds, where topography drives flows, ultimately, it still relies upon the CN to model run-off processes and, therefore, it is limited when applied to the monsoonal Ethiopian Highlands. Water balance models are relatively simple to implement and have been used frequently in the BNB (Johnson and Curtis, 1994; Conway, 1997; Ayenew and Gebreegziabher, 2006; Liu *et al.*, 2008; Kim and Kaluarachchi, 2008; Collick *et al.*, 2009; Steenhuis *et al.*, 2009). Despite their simplicity and improved watershed outlet predictions they fail to predict the spatial location of the run-off generating areas. Collick *et al.* (2009) and, to some degree, Steenhuis *et al.* (2009) present semi-lumped conceptualizations of run-off-producing areas in water balance models. SWAT, a semi-distributed model can predict these run-off source areas in greater detail, assuming the run-off processes are correctly modelled.

Based on the finding discussed above, a modified version of the commonly used SWAT model (White *et al.*, 2011; Easton *et al.*, 2010) is developed and tested. This model is designed to more effectively model hydrological processes in monsoonal climates such as in Ethiopia. This new version of SWAT, including water balance (SWAT-WB), calculates run-off volumes based on the available storage capacity of a soil and distributes the storages across the watershed using a soil topographic wetness index (Easton *et al.*, 2008), and can lead to more accurate simulation of where run-off occurs in watersheds dominated by saturation-excess processes (White *et al.*, 2011). White *et al.* (2011) compared the performance of SWAT-WB and the standard SWAT model in the Gumera watershed in the Lake Tana Basin, Ethiopia, and found that even following an unconstrained calibration of the CN, the SWAT model results were 17–23 per cent worse than the SWAT-WB model results.

Application of models to the watershed, sub-basin and basin scales

Tenaw (2008) used a standard SWAT model for Ethiopian Highlands to analyse the rainfall-run-off process at various scales in the upper BNB. Gelaw (2008) analysed the Ribb watershed using Geographic Information System and analysed the meteorological and data for characterizing the flooding regime and extents of damage in the watershed.

At the sub-basin level, Saliha *et al.* (2011) compared artificial neural network and the distributed hydrological model WaSiM-ETH (where WaSiM is Water balance Simulation Model) for predicting daily run-off over five small to medium-sized sub-catchments in the BNB. Daily rainfall and temperature time series in the input layer and daily run-off time series in the output layer of a recurrent neural net with hidden layer feedback architecture were formed. As most of the watersheds in the basin are ungauaged, Saliha *et al.* (2011) used a Kohonen neural network and WaSiM-ETH to estimate flow in the ungauged basin. Kohonen neural network was used to delineate hydrologically homogeneous regions and WaSiM-ETH was used to generate daily flows. Twenty-five sub-catchments of the BNB in Ethiopia were grouped into five hydrologically homogenous groups. WaSiM was calibrated using automatic nonlinear

parameter estimation (PEST) method coupled with shuffled complex evolution (SCE) algorithm and validated using an independent time series. In the coupled programme, the Kohonen neural network assigns the ungauged catchment into one of the five hydrologically homogeneous groups. Each homogeneous group has its own set of optimized WaSiM-ETH parameters, derived from simultaneous calibration and validation of gauged rivers in the respective homogeneous group. The coupled programme transfers the optimized WaSiM parameters from the homogeneous group (which the ungauged river belongs to) to the ungauged river, and WaSiM calculates the daily flow for this ungauged river.

The two approaches discussed above, developed by Easton *et al.* (2010) and Saliha *et al.* (2011), provided a means of estimating run-off in the BNB across a range of scales and locations. Readers are referred to Saliha *et al.* (2011) for detail models and results on these and the Kohonen neural network and WaSiM-ETH for a detailed discussion. What follows are examples of applications of the SWAT and SWAT-WB at multiple scales in the BNB.

At the watershed level (Gumera), results of a standard SWAT model (Tenaw, 2008) and modified SWAT-WB model (Easton *et al.*, 2010; White *et al.*, 2011) are compared. Tenaw (2008) initialized the standard SWAT model for the Gumera watershed, which provided good calibration results at the monthly time step with a Nash–Sutcliffe efficiency, E_{NS} (Nash and Sutcliffe, 1970), of 0.76, correlation coefficient, R^2, of 0.87, and mean deviation, D, of 3.29 per cent (Figure 6.6). Validation results also show good agreement between measured and simulated values, with E_{NS} of 0.72, R^2 of 0.82 and D of −5.4 per cent.

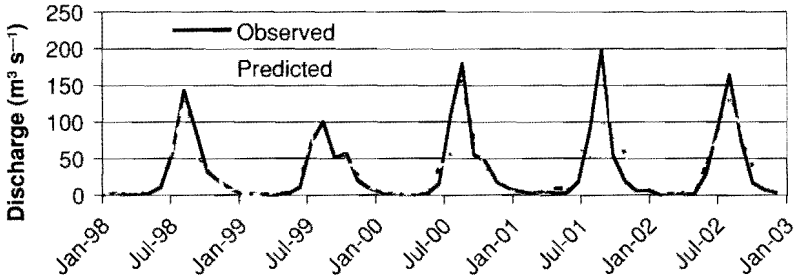

Figure 6.6 Calibration results of average monthly observed and predicted flow at the Gumera gauge using the SWAT

Source: Tenaw, 2008

At the sub-basin level, Habte *et al.* (2007) assessed the applicability of distributed WaSiM-ETH in estimating daily run-off from 15 sub-catchments in the Abbay River Basin. Input data in the form of daily rainfall and temperature data from 38 meteorological stations were used to drive model simulations. In a study by Saliha *et al.* (2011), the artificial neural network and distributed hydrological model (WaSiM-ETH) were compared for predicting daily run-off over five small to medium-sized sub-catchments in the Blue-Nile River Basin. Daily rainfall and temperature time series in the input layer and daily run-off time series in the output layer of recurrent neural net with hidden layer feedback architecture were formed.

The use of neural networks in modelling a complex rainfall–run-off relationship can be an efficient way of modelling the run-off process in situations where explicit knowledge of the internal hydrological process is not available. Indeed, most of the watersheds in the basin are ungauged,

and thus there is little easily available data to run standard watershed models. Saliha *et al.* (2011) used a Self-Organizing Map (SOM) or Kohonen neural network (KNN) and WaSiM-ETH to estimate flow in the ungauged basin. The SOM groupings were used to delineate hydrologically homogeneous regions and WaSiM-ETH was then used to generate daily flows. The 26 sub-catchments of the BNB in Ethiopia were grouped into five hydrologically homogeneous groups, and WaSiM-ETH was then calibrated using the PEST method coupled with the SCE algorithm in neighbouring basins with available data. The results were then validated against an independent time series of flow (Habte *et al.*, 2007). Member catchments in the same homogenous group were split into calibration catchments and validation catchments. Each homogeneous group has a set of optimized WaSiM-ETH parameters, derived from simultaneous calibration and validation of gauged rivers in the respective homogeneous groups. Figure 6.7 shows a general framework of the couple model. In the coupled trained SOM and calibrated WaSiM-ETH programme, the trained SOM will assign the ungauged catchment into one of the five hydrologically homogenous groups based on the pre-defined catchment characteristics (e.g. red broken line in Figure 6.7). The coupled programme then transfers the whole set of optimized WaSiM-ETH parameters from the homogeneous group (to which the ungauged river belongs) to the ungauged river, and WaSiM-ETH calculates the daily flow for this ungauged river.

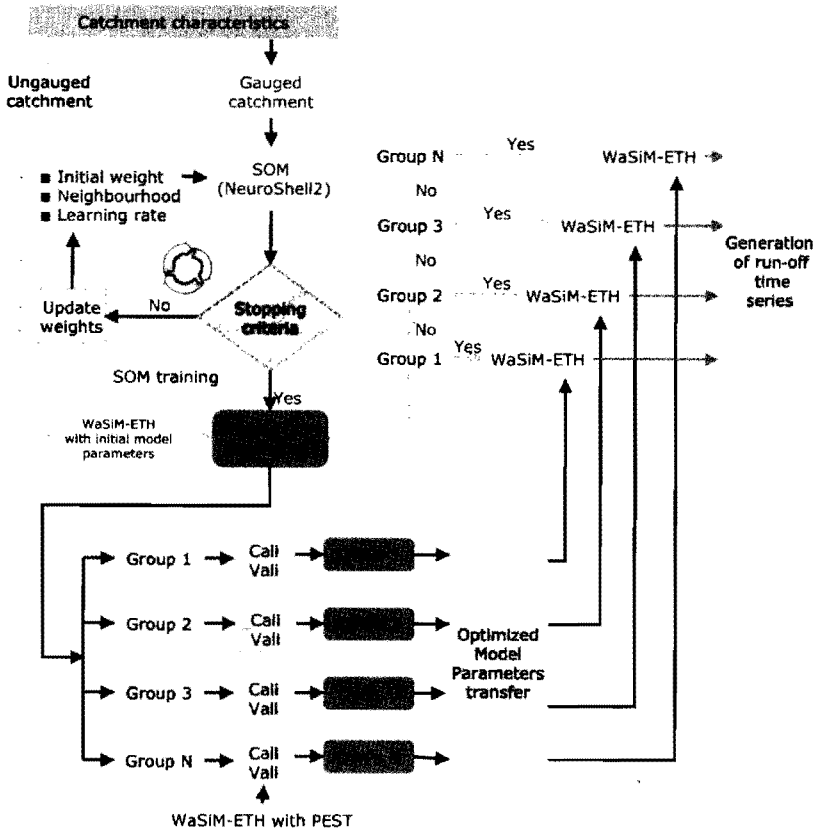

Figure 6.7 Framework of the coupled Water Balance Simulation Model–Ethiopia and Self-Organizing Map models

Source: Saliha *et al.*, 2011

Soil and Water Assessment Tool–Water Balance model

The SWAT-WB model is applied to the Ethiopian portion of the BNB that drains via the main stem of the river at El Diem on the border with Sudan (the Rahad and Dinder sub-basins that drain the north-east region of Ethiopia were not considered; Figures 6.8 and 6.9). Results show that incorporating a redefinition of how hydrological response units (HRUs) are delineated combined with a water balance to predict run-off can improve our analysis of when and where run-off and erosion occur in a watershed. The SWAT-WB model is initialized for eight sub-basins ranging in size from 1.3 to 174,000 km^2. The model is calibrated for flow using a priori

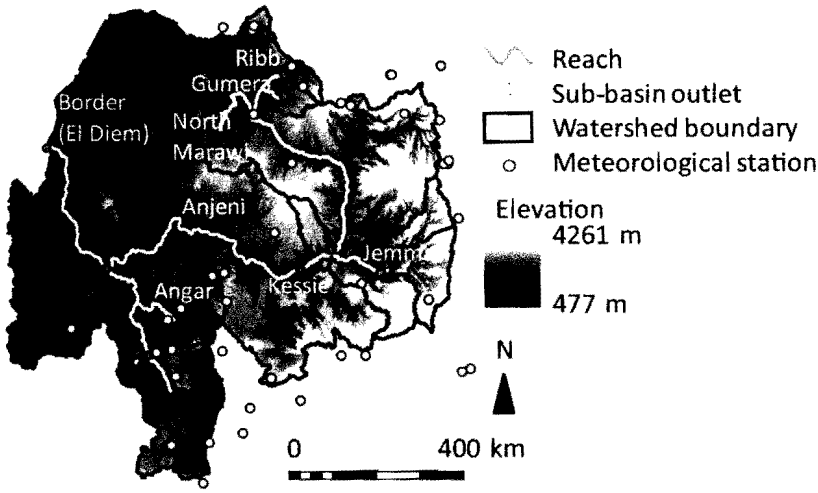

Figure 6.8 Digital elevation model reaches, sub-basins and sub-basin outlets initialized in the Blue Nile Basin SWAT model. Also displayed is the distribution of meteorological stations used in the model

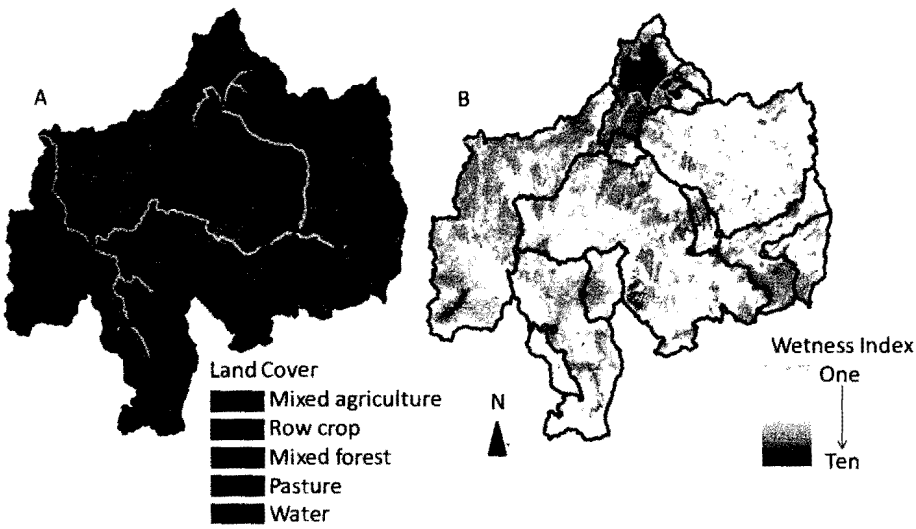

Figure 6.9 Land use/land cover (a) in the Blue Nile Basin (ENTRO) and (b) the Wetness Index used in the Blue Nile SWAT model

topographic information and validated with an independent time series of flows. The tested methodology captures the observed hydrological processes quite well across multiple scales, while significantly reducing the calibration data requirements. The reduced data requirements for model initialization have implications for model applicability to other data-scarce regions. Finally, a discussion of the implications of watershed management with respect to the model results is presented.

Summarized Soil and Water Assessment Tool model description

The SWAT model is a river basin model created to run with readily available input data so that general initialization of the modelling system does not require overly complex data-gathering, or calibration. SWAT was originally intended to model long-term run-off and nutrient losses from rural watersheds, particularly those dominated by agriculture (Arnold *et al.*, 1998). SWAT requires data on soils, land use/management information and elevation to drive flows and direct sub-basin routing. While these data may be spatially explicit, SWAT lumps the parameters into HRUs, effectively ignoring the underlying spatial distribution. Traditionally, HRUs are defined by the coincidence of soil type and land use. Simulations require meteorological input data including precipitation, temperature and solar radiation. Model input data and parameters were parsed using the ARCSWAT 9.2 interface. The interface combines SWAT with the ARCGIS platform to assimilate the soil input map, digital elevation model (DEM) and land use coverage.

Soil and Water Assessment Tool–Water Balance saturation excess model

The modified SWAT model uses a water balance in place of the CN for each HRU to predict run-off losses. Based on this water balance, run-off, interflow and infiltration volumes are calculated. While these assumptions simplify the processes that govern water movement through porous media (in particular, partly saturated regions), for a daily model, water balance models have been shown to better capture the observed responses in numerous African watersheds (Guswa *et al.*, 2002). For Ethiopia, water balance models outperform models that are developed in temperate regions (Liu *et al.*, 2008; Collick *et al.*, 2009; Steenhuis *et al.*, 2009; White *et al.*, 2011). For the complete model description see Easton *et al.*, 2010 and White *et al.*, 2011. In its most basic form, the water balance defines a threshold moisture content over which the soil profile can neither store nor infiltrate more precipitation; thus additional water becomes either run-off or interflow ($q_{if,i}$):

$$q_{if,i} = \begin{cases} (\theta_s - \theta_{i,t})d_i + P_i - Et_i & \text{for: } P_i > (\theta_s - \theta_{i,t})d_i - Et_i \\ 0 & \text{for: } P_i \leq (\theta_s - \theta_{i,t})d_i - Et_i \end{cases} \quad (6.1)$$

where θ_s ($cm^3\ cm^{-3}$) is the soil moisture content above which storm run-off is generated, $\theta_{i,t}$ ($cm^3\ cm^{-3}$) is the current soil moisture content, d_i (mm) is the depth of the soil profile, P_i (mm) is the precipitation and Et_i (mm) is the evapotranspiration. In SWAT, there is no lateral routing of interflow among watershed units, and thus no means to distribute watershed moisture; thus Equation 6.1 will result in the same excess moisture volume everywhere in the watershed given similar soil profiles.

To account for the differences in run-off generation in different areas of the basin, the following threshold function for storm run-off that varies across the watershed as a function of topography is used (Easton *et al.*, 2010):

$$\tau_i + (\rho_i \theta s - \theta_{i,i}) \tag{6.2}$$

where, ρ_i is a number between 0 and 1 that reduces θ_s to account for water that should drain down slope, and is a function of the topography (as defined by a topographic wetness index, λ; e.g. Beven and Kirkby, 1979). Here it is assumed that the distribution of ρ_i values is inversely proportional to the soil topographic index (λ_i) averaged across each wetness index class or HRU and that the lowest λ, (λ_o) corresponds to the highest λ_i (λ_o):

$$\rho_i = \frac{\lambda_o}{\lambda_i} \tag{6.3}$$

Easton *et al.* (2010) showed that using the baseflow index reliably constrained the distribution of these ρ_i values. Note that Equation 6.2 applies only to the first soil layer. Once the soil profile has been adequately filled, Equation 6.2 can be used to write an expression for the depth of run-off, $q_{R,i}$ (mm) from a wetness index, i:

$$q_{R,i} = \begin{cases} P_i - \tau_i d_i & \text{for } P_i > \tau_i d_i \\ 0 & \text{for } P_i \leq \tau_i d_i \end{cases} \tag{6.4}$$

While the approach outlined above captures the spatial patterns of VSAs and the distribution of run-off and infiltrating fractions in the watersheds, Easton *et al.* (2010) noted there is a need to maintain more water in the wettest wetness index classes for evapotranspiration, and proposed adjusting of the available water content (*AWC*) of the soil layers below the first soil layer (recall that the top soil layer is used to establish our run-off threshold; Equation 6.2) so that higher topographic wetness index classes retain water longer (i.e. have *AWC* adjusted higher), and the lower classes dry faster (i.e. *AWC* is adjusted lower by normalizing by the mean ρ_i value, similar to Easton *et al.*, 2008, for example).

Note that, since this model generates run-off when the soil is above saturation, total rainfall determines the amount of run-off. When results are presented on a daily basis rainfall intensity is assumed to be inconsequential. It is possible that under high-intensity storms (e.g. storms with rainfall intensities greater than the infiltration capacity of the soil) the model might under-predict the amount of run-off generated, but this is the exception rather than the rule (Liu *et al.*, 2008; Engda, 2009).

Model calibration

The water balance methodology requires very little direct calibration, as most parameters can be determined a priori. Soil storage was calculated as the product of soil porosity and soil depth from the soils data. Soil storage values were distributed via the λ described above, and the effective depth coefficient (ρ_i, varies from 0 to 1) was adjusted along a gradient in λ values as in Equation 6.3. Here it is assumed that the distribution of λ_i values is inversely proportional to λ_i (averaged across each wetness index class or HRU) and that the lowest λ, (λ_o) corresponds to the highest λ_i (λ_o). In this manner, the ρ_i distribution requires information on the topography (and perhaps on soil). If a streamflow record is available baseflow separation can be employed to further parameterize the model.

In constraining or 'calibrating' ρ_i, it is recognized that, since the ρ-value controls how much precipitation is routed as run-off, it also controls how much precipitation water can enter the soil for a given wetness index class. Thus, a larger fraction of the precipitation that falls on an

Table 6.2 Effective depth coefficients (ρ_i) for each wetness index class and watershed in the Blue Nile Basin model from Equation 6.3. The ΠB is determined from baseflow separated run-off of the streamflow hydrograph and distributed via the topographic wetness index, λ

Wetness index class	ρ_i *(Border)*	ρ_i *(Kessie)*	ρ_i *(Jemma)*	ρ_i *(Angar)*	ρ_i *(Gumera)*	ρ_i *(Ribb)*	ρ_i *(N. Marawi)*	ρ_i *(Anjeni)*
10 (most saturated)	0.22	0.20	0.16	0.15	0.26	0.24	0.24	0.15
9	0.58	0.51	0.24	0.22	0.31	0.41	0.43	0.25
8	0.75	0.68	0.31	0.26	0.40	0.51	0.53	0.30
7	0.87	0.78	0.35	0.30	0.47	0.59	0.62	0.32
6	0.97	0.87	0.37	0.34	0.61	0.66	0.69	0.36
5	1.00	0.94	0.43	0.38	0.75	0.72	0.75	0.44
4	1.00	1.00	0.57	0.42	0.89	0.80	0.83	0.46
3	1.00	1.00	0.64	0.47	1.00	0.88	0.91	0.57
2	1.00	1.00	0.74	0.52	1.00	0.99	1.00	0.86
1 (least saturated)	1.00	1.00	1.00	0.63	1.00	1.00	1.00	1.00
$*\Pi_B$	**0.84**	**0.80**	**0.48**	**0.37**	**0.67**	**0.68**	**0.70**	**0.47**

Note: $*\Pi_B$ partitions moisture in the above saturation to run-off and infiltration

area with a large ρ_i will potentially recharge the groundwater than in an area with a small ρ_i. As a first approximation, then, assume ρ_i can be equated with the ratio of groundwater recharge, $q_{B,i}$ to total excess precipitation, $q_{t,i}$ (i.e. precipitation falling on wetness class i that eventually reaches the watershed outlet). Baseflow is determined directly from the digital signal filter baseflow separation technique of several years of daily streamflow hydrographs (Hewlett and Hibbert, 1967; Arnold *et al.*, 1995; for greater detail see Easton *et al.*, 2010).

The primary difference between the CN-based SWAT and the water-balance-based SWAT is that run-off is explicitly attributable to source areas according to a wetness index distribution, rather than by land use and soil infiltration properties as in original SWAT (Easton *et al.*, 2008). Soil properties that control saturation-excess run-off generation (saturated conductivity, soil depth) affect run-off distribution in SWAT-WB since they are included in the wetness index via Equation 6.4. Flow calibration was validated against an independent time series that consisted of at least one half of the observed data. To ensure good calibration, the calibrated result maximized the coefficient of determination (r^2) and the Nash–Sutcliffe efficiency (E_{NS}; Nash and Sutcliffe, 1970). Table 6.2 summarizes the calibrated ρ_i values for each wetness index class while Table 6.3 summarizes the calibration statistics. Since flow data at some of the available gauge locations were available at the monthly time step (Angar, Kessie, Jemma) and daily at others (Anjeni, Gumera, Ribb, North Marawi, El Diem; Figure 6.10), the model was run for both time steps, and the results presented accordingly.

Results

Run-off from saturated areas and subsurface flow from the watershed were summed at the watershed outlet to predict streamflow. The graphical comparison of the modelled and measured daily streamflow at the El Diem station at the Sudan border (e.g. integrating all sub-basins above) is shown in Figure 6.10. The model was able to capture the dynamics of the basin

response well (E_{NS} = 0.87, r^2 = 0.92; Table 6.3; Figure 6.10). Both baseflow and storm flow were correctly predicted with a slight over-prediction of peak flows and a slight under-prediction of low flows (Table 6.3); however, all statistical evaluation criteria indicated the model predicted well. In fact, all calibrated sub-basins predicted streamflow at the outlet reasonably well (e.g. Table 6.3). Model predictions showed good accuracy (E_{NS} ranged from 0.53 to 0.92) with measured data across all sites except at Kessie, where the water budget could not be closed; however, the timing of flow was well captured. The error at Kessie appears to be due to under-estimated precipitation at the nearby gauges, as measured flow was nearly 15 per cent higher than precipitation – evapotranspiration (P – E). Nevertheless, the prediction is within 25 per cent of the measured data. Observed normalized discharge (Table 6.3) across the sub-basins shows a large gradient, from 210 mm at Jemma to 563 mm at Anjeni. For the basin as a whole, approximately 25 per cent of precipitation exits at El Diem of the BNB.

Table 6.3 Calibrated sub-basins (Figure 6.10), drainage area, model fit statistics (coefficient of determination, r^2 and Nash–Sutcliffe Efficiency, E_{NS}), and observed and predicted flows

Sub-basin	*Area (km^2)*	r^2	E_{NS}	*Observed mean annual discharge (million m^3)*	*Observed normalized discharge (mm yr^{-1})*	*Predicted direct run-off ($mmyr^{-1}$)*	*Predicted ground-water ($mmyr^{-1}$)*[3]
Anjeni[1]	1.3	0.76	0.84	0.40	563	44	453
Gumera[1]	1286	0.83	0.81	501	390	22	316
Ribb[1]	1295	0.74	0.77	495	382	25	306
North Marawi[1]	1658	0.78	0.75	646	390	17	274
Jemma[2]	5429	0.91	0.92	1142	210	19	177
Angar[2]	4674	0.87	0.79	1779	381	34	341
Kessie[2]	65,385	0.73	0.53	19,237	294	19	259
Border (El Diem)[1]	174,000	0.92	0.87	56,021	322	13	272

Notes: [1] Statistics are calculated on daily time step
[2] Statistics are calculated on monthly time step
[3] Includes both baseflow and interflow

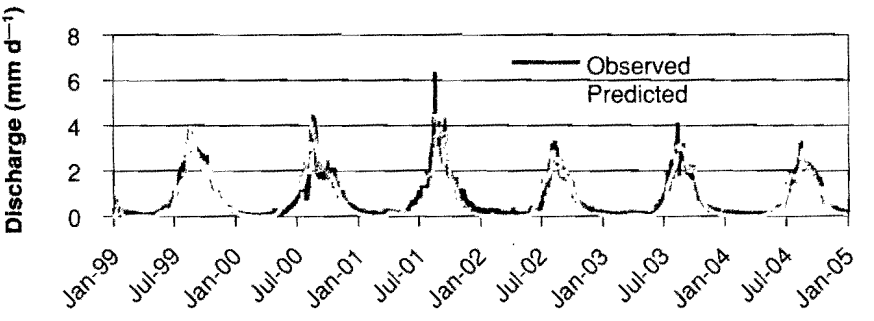

Figure 6.10 Daily observed and predicted discharge at the Sudan border

Table 6.2 shows the adjusted ρ_i parameter values (e.g. Equation 6.3) for the various sub-basins in the BNB; these values are scalable, and can be determined from topographical information (i.e. the ρ_i values vary by sub-basin, but the distribution is similar).

The SWAT-WB model was able to accurately reproduce the various watershed responses across the range of scales. Notice, for instance, that the hydrographs at the Sudan border (174,000 km^2; Figure 6.12), Gumera (1200km^2; Figure 6.11) and Anjeni (1.13km^2; Figure 6.12) reasonably capture the observed dynamics (i.e. both the rising and receding limbs and the peak flows are well represented). There was a slight tendency for the model to bottom out during baseflow, probably due to overestimated ET, but the error is relatively minor. More importantly, the model captures peak flows, which are critical to correctly predict to assess sediment transport and erosion.

Run-off and streamflow are highly variable both temporally (over the course of a year; Figure 6.10) and spatially (across the Ethiopian Blue Nile Basin; Table 6.3). Daily watershed outlet discharge during the monsoonal season at Gumera is four to eight times larger than at the Sudan border (after normalizing flow by the contributing area; Figures 6.10 and 6.11). Anjeni, the smallest watershed had the largest normalized discharge, often over 20 mm d^{-1} during the rainy season (Figure 6.12). Discharges (in million m^3 y^{-1}) intuitively increase with drainage area, but precipitation also has a large impact on overall sub-basin discharge. Both Jemma and Angar are of approximately the same size (Jemma is actually slightly bigger), yet discharge from Angar is nearly 40 per cent higher, a result of the higher precipitation in the southwestern region of the basin. Temporally, outlet discharges typically peak in August for the small and medium-sized basins and slightly later for Kessie and the Sudan border, a result of the lag time for lateral flows to travel the greater distances. Due to the monsoonal nature of the basin, there is a very low level of baseflow in all tributaries and, in fact, some dry up completely during the dry season, which the model reliably predicts, which is important when considering the impacts of intervention measures to augment flow.

Run-off losses predicted by the model varied across the basin as well, and were generally well corroborated by run-off estimates from baseflow separation of the streamflow hydrograph. Predicted run-off losses (averaged across the entire sub-basin) varied from as low as 13 mm y^{-1} for the BNB as a whole sub-basin to as high as 44 mm y^{-1} in Anjeni. Of course, small areas of

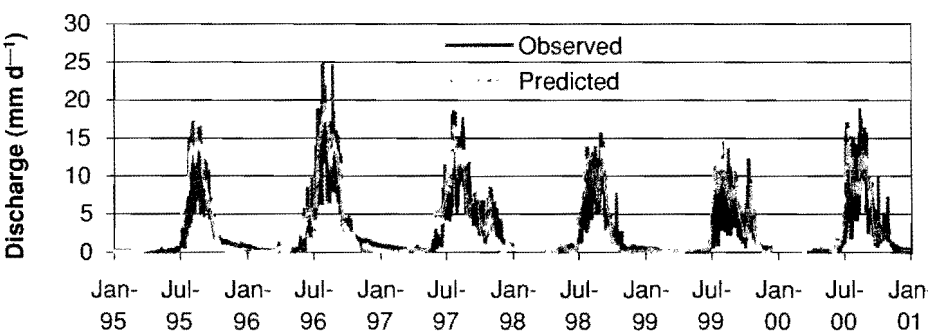

Figure 6.11 Daily observed and predicted discharge from the Gumera sub-basin. See Table 6.3 for model performance for the Ribb and North Marawi sub-basins

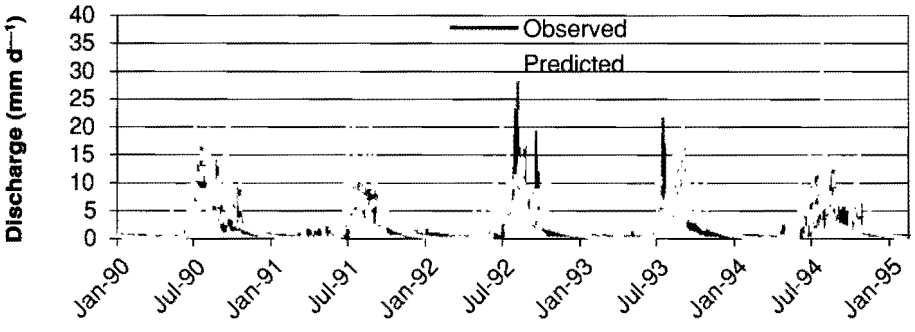

Figure 6.12 Daily observed and predicted discharge from the Anjeni micro-watershed

the individual sub-basins produce significantly higher run-off losses and others significantly less. These differences are well reflected in the average baseflow coefficient (Π_{bi}) for the sub-basins (Table 6.2). Notice that Π_B for Anjeni (smallest watershed, highest run-off losses) is significantly lower than for Gumera and the Sudan border (Table 6.2). A lower Π_B reflects less average available storage in the watershed (i.e. more rainfall ends up as run-off). This Π_B value is determined from the baseflow separation of the streamflow hydrograph (Hewlett and Hibbert, 1967), and can thus be considered a measured parameter. It is also interesting to note how the distribution of the individual ρ_i differs between basins. For instance, there are more classes (areas) in Anjeni and Angar that are prone to saturate, and would thus have lower available storage, and create more run-off. This is relatively clear in looking at the streamflow hydrographs (Figures 6.10–6.13) where the smaller watersheds tend to generate substantially more surface run-off. Conversely, as basin size increases (Kessie, Sudan border) the saturated fraction of the watershed decreases, and more of the rainfall infiltrates, resulting in greater baseflow, as reflected in the higher Π_B, or, in terms of run-off, the smaller upland watersheds have higher run-off losses than the larger basins. This is not unexpected, as the magnitude of the subsurface flow paths have been shown to increase with the size of the watershed, because as watershed size increases more and more deep flow paths become activated in transport (Steenhuis *et al.*, 2009).

The ability to predict the spatial distribution of run-off source areas has important implications for watershed intervention, where information on the location and extent of source areas is critical to effectively managing the landscape. For instance, the inset of Figure 6.13 shows the predicted spatial distribution of average run-off losses for the Gumera watershed for an October 1997 event. As is evident from Figure 6.13, run-off losses vary quite dramatically across the landscape; some HRUs are expected to produce no run-off, while others have produced more than 90 mm of run-off. When averaged spatially at the outlet, run-off losses were 22 mm (Table 6.3). Other sub-basins responded in a similar manner. These results are consistent with data collected in the Anjeni SCRP watershed (SCRP, 2000; Ashagre, 2009), which show that run-off losses roughly correlate with topography.

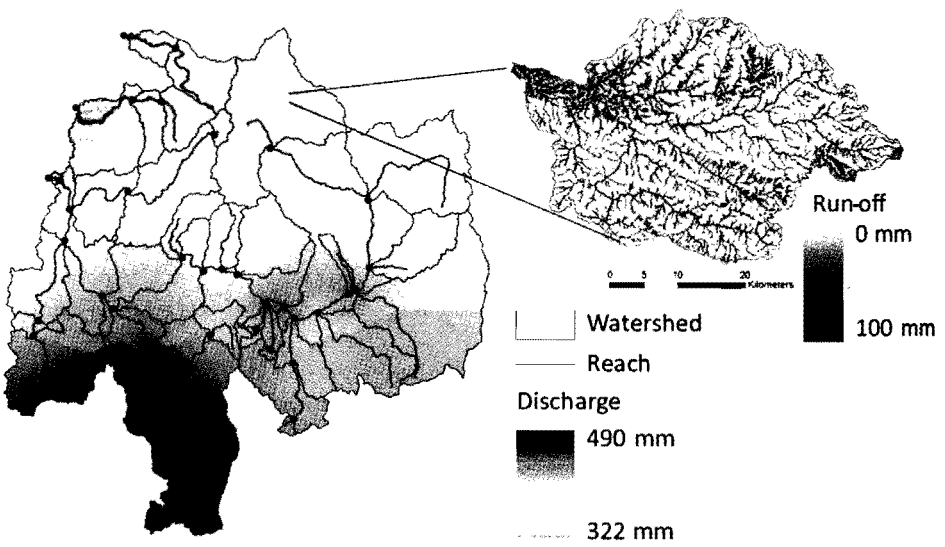

Figure 6.13 Predicted average yearly spatial distribution of discharge in the BNB (main) and predicted run-off distribution in the Gumera sub-watershed for an October 1997 event (inset)

Discussion

Flows in the Blue Nile Basin in Ethiopia show large variability across scales and locations. Sediment and water yields from areas of the basin range more than an order of magnitude (a more in-depth discussion of sediment is given in Chapter 7). The use of the modified SWAT-WB model that more correctly predicts the spatial location of run-off source areas is a critical step in improving the ability to manage landscapes, such as the Blue Nile, to provide clean water supplies, enhance agricultural productivity and reduce the loss of valuable topsoil. Obviously, the hydrological routines in many of the large-scale watershed models do not incorporate the appropriate mechanistic processes to reliably predict when and where run-off occurs, at least at the scale needed to manage complex landscapes. For instance, the standard SWAT model predicts run off to occur more or less equally across the various land covers (e.g. croplands produce approximately equal run-off losses and pastureland produces approximately equal erosive losses, etc.) provided they have similar soils and land management practices throughout the basin. The modified version of SWAT used here recognizes that different areas of a basin (or landscape) produce different run-off losses and thus different sediment losses. However, all crops or pasture within a wetness index class in the modified SWAT produce the same run-off or erosion losses.

Water balance models are consistent with the saturation excess run-off process because the run-off is related to the available watershed storage capacity and the amount of precipitation. The implementation of water balances into run-off calculations in the BNB is not a novel concept and others have shown that water balance type models often perform better than more complicated models in Ethiopian-type landscapes (Johnson and Curtis, 1994; Conway, 1997; Liu *et al.*, 2008). However, these water balance models are typically run on a monthly or yearly time steps because the models are generally not capable of separating base-, inter- and surface run-off flow. To truly model erosion and sediment transport (of great interest in the BNB), large events

must be captured by the model and daily simulations are required to do so. Thus SWAT-WB not only maintains a water balance but also calculates the interflow and the baseflow component, and gives a reasonable prediction of peak flows. SWAT-WB is therefore more likely to be capable of predicting erosion source areas and sediment transport than either SWAT-CN or water budget models with monthly time steps. Indeed, Tebebu *et al.* (2010) found gully formation and erosion in the Ethiopian Highlands to be related to water table levels and saturation dynamics, which SWAT-WB reliably predicts.

Conclusions

A modified version of the SWAT model appropriate for monsoonal climates is presented as a tool to quantify the hydrological and sediment fluxes in the BNB, Ethiopia. The model requires very little direct calibration to obtain good hydrological predictions. All parameters needed to initialize the model to predict run-off are obtained from baseflow separation of the hydrograph (Π_B), and from topographical information derived from a DEM and soils data (λ). The reduced parameterization/calibration effort is valuable in environments such as Ethiopia where limited data are available to build and test complicated biogeochemical models.

The model quantified the relative contributions from the various areas of the BNB with relatively good accuracy, particularly at a daily time step. The analysis showed that not all sub-basins contribute flow or run-off equally. In fact, there is large variation in average flow and run-off across the watershed. Additionally, within any one watershed the model indicates that there are areas that produce significantly more run-off and areas that produce almost no run-off, which, of course, has implications for the management of these areas. This model is helpful to identify areas of a basin that are susceptible to erosive or other contaminant losses, due to high run-off production. These areas should be targeted for management intervention to improve water quality.

References

Arnold, J. G., Allen, P. M., Muttiah, R. and Bernhardt G. (1995) Automated base-flow separation and recession analysis techniques, *Ground Water*, 33, 1010–1018.

Arnold, J. G., Srinivasan, R., Muttiah, R. S. and Williams, J. R. (1998) Large area hydrologic modelling and assessment part I: model development, *Journal of the American Water Resources Association*, 34, 1, 73–89.

Arseno, Y. and Tanırat, I. (2005) Ethiopia and the eastern Nile Basin, *Aquatic Sciences*, 16, 15–27.

Ashagre, B. B. (2009) Formulation of best management option for a watershed using SWAT (Anjeni watershed, Blue Nile Basin, Ethiopia), MPS thesis, Cornell University, Ithaca, NY.

Bekele, S. and Horlacher, H. H. B. (2000) Development and application of 2-parameter monthly water balance model in limited data situation: the case of Abaya-Chamo Basin, Ethiopia, *Zede (Ethiopian Journal of Engineers and Architects)*, 17, 56–79.

Awulachew, S. B., Yilma, A. D., Luelseged, M., Loiskandl, W., Ayana, M. and Alamirew, T. (2007) *Water Resources and Irrigation Development in Ethiopia*, Working paper 123, International Water Management Institute, Colombo, Sri Lanka.

Ayenew, T. and Gebreegziabher, Y. (2006) Application of a spreadsheet hydrological model for computing long-term water balance of Lake Awassa, Ethiopia, *Hydrological Sciences*, 51, 3, 418–431.

Bayabil, H. K. (2009) Are runoff processes ecologically or topographically driven in the (sub) humid Ethiopian Highlands? The case of the Maybar watershed, MPS thesis, Cornell University, Ithaca, NY.

Beven, K. J. and Kirkby, M. J. (1979) Towards a simple physically-based variable contributing model of catchment hydrology, *Hydrological Science Bulletin*, 24 1, 43–69.

Bosshart, U. (1997) *Measurement of River Discharge for the SCRP Research Catchments: Gauging Station Profiles*, Soil Conservation Reserve Program, Research reports 31, University of Bern, Bern, Switzerland.

Bryant, R. D., Gburek, W. J., Veith, T. L. and Hively, W. D. (2006) Perspectives on the potential for hydropedology to improve watershed modeling of phosphorus loss, *Geoderma*, 131, 299–307.

Collick, A. S., Easton, Z. M., Adgo, E., Awulachew, S. B., Gete, Z. and Steenhuis, T. S. (2009) Application of a physically-based water balance model on four watersheds throughout the upper Nile basin in Ethiopia, *Hydrological Processes*, 23, 3718–372.

Conway, D. (1997) A water balance model of the upper Blue Nile in Ethiopia, *Hydrological Sciences*, 42, 2, 265–286.

Conway, D. and Hulme, M. (1993) Recent fluctuations in precipitation and runoff over the Nile sub-basins and their impact on main Nile discharge, *Climatic Change*, 25, 127–151.

Derib, S. D. (2005) Rainfall-runoff processes at a hill-slope watershed: case of simple models evaluation at Kori-Sheleko catchments of Wollo, Ethiopia, MSc thesis, Wageningen University, The Netherlands.

Easton, Z. M., Fuka, D. R., Walter, M. T., Cowan, D. M. Schneiderman, E. M. and Steenhuis, T. S. (2008) Re-conceptualizing the Soil and Water Assessment Tool (SWAT) model to predict runoff from variable source areas, *Journal of Hydrology*, 348, 3–4, 279–291.

Easton, Z. M., Fuka, D. R., White, E. D., Collick, A. S., Ashagre, B. B., McCartney, M., Awulachew, S. B., Ahmed, A. A. and Steenhuis, T. S. (2010) A multibasin SWAT model analysis of runoff and sedimentation in the Blue Nile, Ethiopia, *Hydrology and Earth System Sciences*, 14, 1827–1841.

Engda, T. A. (2009) Modeling rainfall, runoff and soil loss relationships in the northeastern Highlands of Ethiopia, Andit Tid watershed, MPS thesis, Cornell University, Ithaca, NY.

Gelaw, S. (2008) Causes and impacts of flooding in Ribb river catchment, MSc thesis, School of Graduate Studies Department of Geography and Environmental Studies, Addis Ababa University, Addis Ababa, Ethiopia.

Grunwald, S. and Norton, L. D. (2000) Calibration and validation of a non-point source pollution model, *Agricultural Water Management*, 45, 17–39.

Guswa, A. J., Celia, M. A. and Rodriguez-Iturbe, I. (2002) Models of soil dynamics in ecohydrology: a comparative study, *Water Resources Research*, 38, 9, 1166–1181.

Habte, A. S., Cullmann, J. and Horlacher, H. B. (2007) Application of WaSiM distributed water balance simulation model to the Abbay River Basin, FWU, *Water Resources Publications*, 6, 1613–1045.

Hawkins, R. H. (1979) Runoff curve numbers from partial area watersheds, *Journal of Irrigation, Drainage and Engineering–ASCE*, 105, 4, 375–389.

Hewlett, J. D. and Hibbert, A. R. (1967) Factors affecting the response of small watersheds to precipitation in humid area, in *Proceedings of International Symposium on Forest Hydrology*, W. E. Sopper and H. W. Lull (eds), pp275–290, Pergamon Press, Oxford, UK.

Horton, R. E. (1940) An approach toward a physical interpretation of infiltration capacity, *Soil Science Society of America Proceedings*, 4, 399–418.

Hu, C. H., Guo, S. L., Xiong, L. H. and Peng, D. Z. (2005) A modified Xinanjiang model and its application in northern China, *Nordic Hydrology*, 3, 175–192.

Hurni, H. (1984) *The Third Progress Report*, Soil Conservation Reserve Program, vol 4, University of Bern and the United Nations University, Ministry of Agriculture, Addis Ababa, Ethiopia.

Ibrahim, A. M. (1984) The Nile – Description, hydrology, control and utilization, *Hydrobiologia*, 110, 1–13.

Johnson, P. A. and Curtis, P. D. (1994) Water balance of Blue Nile river basin in Ethiopia, *Journal of Irrigation, Drainage and Engineering–ASCE*, 120, 3, 573–590.

Kim, N. W. and Lee, J. (2008) Temporally weighted average curve number method for daily runoff simulation, *Hydrological Processes*, 22, 4936–4948.

Kim, U. and Kaluarachchi, J. J. (2008) Application of parameter estimation and regionalization methodologies to ungauged basins of the upper Blue Nile river basin, Ethiopia, *Journal of Hydrology*, 362, 39–56.

Lange, J., Greenbaum, N., Husary, S., Ghanem, M., Leibundgut, C. and Schick, A. P. (2003) Runoff generation from successive simulated rainfalls on a rocky, semi-arid, Mediterranean hillslope, *Hydrological Processes*, 17, 279–296.

Liu, B. M., Collick, A. S., Zeleke, G., Adgo, E., Easton, Z. M. and Steenhuis, T. S. (2008) Rainfall-discharge relationships for a monsoonal climate in the Ethiopian highlands, *Hydrological Processes*, 22, 7, 1059–1067.

Lyon, S. W., Walter, M. T., Gerard-Marchant, P. and Steenhuis, T. S. (2004) Using a topographic index to distribute variable source area runoff predicted with the SCS curve-number equation, *Hydrological Processes*, 18, 2757–2771.

McHugh, O. V. (2006) Integrated water resources assessment and management in a drought-prone watershed in the Ethiopian highlands, PhD thesis, Department of Biological and Environmental Engineering, Cornell University, Ithaca, NY.

Merz, J., Dangol, P. N., Dhakal, M. P., Dongol, B. S., Nakarmi, G. and Weingartner, R. (2006) Rainfall-runoff events in a middle mountain catchment of Nepal, *Journal of Hydrology*, 331, 3–4, 446–458.

MoWR (Ministry of Water Resources) (2002) *Ethiopian Water Sector Strategy*, MoWR, Addis Ababa, Ethiopia.

Nash, J. E. and Sutcliffe, J. V. (1970) River flow forecasting through conceptual models, Part I a discussion of principles, *Journal of Hydrology*, 10, 282–290.

Nyssen, J., Clymans, W., Descheemaeker, K., Poesen, J., Vandecasteele, I., Vanmaercke, M., Zenebe, A., Camp, M.V., Mitiku, H., Nigussie, H., Moeyersons, H., Martens, K., Tesfamichael, G., Deckers, J. and Walraevens, K. (2010) Impact of soil and water conservation measures on catchment hydrological response – a case in north Ethiopia, *Hydrological Processes*, 24, 13, 1880–1895.

Saliha, A. H., Awulachew, S. B., Cullmann, J. and Horlacher, H. B. (2011) Estimation of flow in ungauged catchments by coupling a hydrological model and neural networks: case study, *Hydrological Research*, 42, 5, 386–400.

Schneiderman, E. M., Steenhuis, T. S., Thongs, D. J., Easton, Z. M., Zion, M. S., Neal, A. L., Mendoza, G. F. and Walter, M. T. (2007) Incorporating variable source area hydrology into a curve-number-based watershed model, *Hydrological Processes*, 21, 3420–3430.

SCRP (Soil Conservation Reserve Program) (2000) *Area of Anjeni, Gojam, Ethiopia: Long-Term Monitoring of the Agricultural Environment 1984–1994*, 2000 Soil Erosion and Conservation Database, Soil Conservation Reserve Program, Centre for Development and Environment, Berne, Switzerland in association with the Ministry of Agriculture, Addis Ababa, Ethiopia.

Sheridan, J. M. and Shirmohammadi, A. (1986) Application of curve number procedure on coastal plain watersheds, in *Proceedings from the 1986 Winter Meeting of the American Society of Agricultural Engineers*, paper no. 862505, American Society of Agricultural Engineers, Chicago, IL.

Steenhuis, T. S., Collick, A. S., Easton, Z. M., Leggesse, E. S., Bayabil, H. K., White, E. D., Awulachew, S. B., Adgo, E. and Ahmed, A. A. (2009) Predicting discharge and erosion for the Abay (Blue Nile) with a simple model, *Hydrological Processes*, 23, 3728–3737.

Steenhuis, T. S., Winchell, M., Rossing, J., Zollweg, J. A. and Walter, M. F. (1995) SCS runoff equation revisited for variable-source runoff areas, *Journal of Irrigation, Drainage and Engineering–ASCE*, 121, 3, 234–238.

Sutcliffe, J. V. and Parks, Y. P. (1999) *The Hydrology of the Nile*, Special Publication 5, IAHS, Wallingford, UK, p180.

Tebebu, T. Y. (2009) Surface and subsurface flow effects on permanent gully formation and upland erosion near Lake Tana in the northern Highlands of Ethiopia, MPS thesis, Cornell University, Ithaca, NY.

Tebebu, T. Y., Abiy, A. Z., Dahlke, H. E., Easton, Z. M., Zegeye, A. D., Tilahun, S. A., Collick, A. S., Kidnau, S., Moges, S., Dadgari, F. and Steenhuis, T. S. (2010) Surface and subsurface flow effects on permanent gully formation and upland erosion near Lake Tana in the northern Highlands of Ethiopia, *Hydrological Earth System Sciences*, 14, 2207–2217.

Tenaw, A. (2008) SWAT based run off and sediment yield modeling (a case study of Gumera watershed in Lake Tana sub basin), Ethiopia, MSc thesis, Arba Minch University, Ethiopia.

Wang, X., Shang, S., Yang, W. and Melesse, A. M. (2008) Simulation of an agricultural watershed using an improved curve number method in SWAT, *Transactions of the ASAE*, 51, 4, 1323–1339.

White, E. D., Easton, Z. M., Fuka, D. R., Collick, A. S., Adgo, E., McCartney, M., Awulachew, S. B., Selassie, Y. G. and Steenhuis, T. S. (2011) Development and application of a physically based landscape water balance in the SWAT model, *Hydrological Processes*, 25, 15–25.

White, E. D., Feyereisen, G. W., Veith, T. L. and Bosch, D. D. (2009) Improving daily water yield estimates in the Little River watershed: SWAT adjustments, *Transactions of the ASAE*, 52, 1, 69–79.